

## NUMERICAL AND EXPERIMENTAL ANALYSIS OF A SHEAR-LINK ENERGY DISSIPATOR FOR SEISMIC PROTECTION OF BUILDINGS

Francisco Hurtado<sup>1</sup> and Luis M. Bozzo<sup>2</sup>

<sup>1</sup>University of Michoacán (UMSNH), Civil Engineer School, Structures Department,  
58000 Morelia Michoacán, México

<sup>2</sup>Luis Bozzo Projects and Structures, S.L, 08009 Barcelona, Spain  
Email: [fco.hsoto@gmail.com](mailto:fco.hsoto@gmail.com), [lbozrot@ciccp.es](mailto:lbozrot@ciccp.es)

### ABSTRACT :

This paper presents the numerical analysis and the experimental results of an energy dissipator based on metal yielding for seismic protection of buildings. The study is oriented to propose a *Shear-Link* device that exhibits yielding when experiencing small displacements and to evaluate its experimental behavior. It is presented the numerical model of the proposed device and their force-displacement relation-ship, as well as the results of the device hysteretic characterization test when applying monotonic growing load. The corresponding force-displacement relation-ship is obtained to validate the numerical model. The experimental model was manufactured with conventional structural steel. Its shape in wide-flange section allows an optimum energy dissipation in the whole section besides being very stable provided web buckling is avoided. Its behavior therefore is similar to that of eccentric bracing. The results were generalized in 32 different units with yielding force between 13.65 kN and 435.5 kN. All these units had yielding displacement around 0.25 mm.

**KEYWORDS:** Shear, Link, Energy, Dissipator

### 1. INTRODUCTION

In the last decades a lot of the investigation carried out on the structural behavior of buildings in seismic areas, has been focused to the development of seismic control systems, as much for the seismic design of new constructions as for the buildings rehabilitation damaged by these phenomena. All This, like an alternative to the conventional seismic design, based on the concepts of ductility and structural redundancy, that allows significant reduction in the forces induced by a severe earthquake. However, with the reduction of these forces, it is being accepted that the structure can suffer damages of certain magnitude when an intense earthquake is presented, since the structure can work in the non linear range with the consequent yielding of some of its elements. The above mentioned, originates the appearance of permanent deformations, which usually generates damages in the structural and non structural elements, especially in those structures that have low ductility, or they are very flexible.

The systems of structural control, contrary to the above mentioned, concentrate the damages that can be presented by the action of a severe earthquake on certain elements or connections that can be easily replaced and which failure do not put in danger the global security of the structures. These systems may also deviate the seismic movement effect from the structure to other elements designed specially for it, so that the vibrations originated by the action of the earthquake, do not damage the constructions which may be dampen, without damaging the main structure.

### 2. "SL" DISSIPATORS DESCRIPTION AND CHARACTERISTICS

The proposed *Shear-Link* dissipator is based on the eccentric braces structural system since the overall shape is

a well stiffened wide-flange section (see figure 4 and 5). However, the system is not based on standard shapes or specially welded ones. Instead the device is milled from a plane standard shape. This fabrication process proposed by Cahís (1998) allows very thin dissipative areas without welding. In the other hand, as in eccentric braces, dissipation of energy is uniform in the whole section, and it is very stable provided web buckling is avoided. Another important feature of the SL dissipator is that it presents a double mode work. Initially the energy is dissipated mainly in the web by uniform shear stresses in a “shear mode”. After the web degrades the stiffeners continue dissipating energy in a “flexural mode”. The deflected shape changes significantly among those modes from a linear one to a curved one. The importance of this feature is that it provides a robust system that continues dissipating energy even after the web is degraded. Even though the design of the connection counts only the first working mode, the second one provides an additional safety factor.

### 3. NUMERICAL PLASTICITY ANALYSIS

To define the optimum shape and characteristics of the dissipator, four basic preliminary devices called Disip1SL30\_2, Disip2SL30\_2, Disip3SL30\_2 and Disip4SL30\_2, have been compared. All have in common two vertical stiffeners (20 mm width) at both lateral ends, the width is 300 mm, the web thickens 2mm and the initial plate thickness 20 mm. The first device has 200 mm height and just one 10 mm vertical stiffener (besides the two at the ends just indicated). Consequently this device has two milled areas of 125x200 mm. The second device adds an horizontal 10 mm stiffener, so the milled areas are 125x95 mm. The objective is to increase their strength against web buckling. In this line the third device has two horizontal stiffeners, so the milled areas are 125x60 mm. The last preliminary device reduces the vertical height up to 110 mm maintaining a horizontal stiffener. The dimensions for this device is presented in figure 4.

The plastic nonlinear analysis has been performed using the computer program ANSYS. The model for all the cases corresponds to the isotropic hardening one giving the complete stress – strain material relation. This relation was obtained experimentally for a typical material. Figure 1 shows the Von Mises stresses for a given imposed relative displacement of 20 mm for the devices Disip3SL30\_2 and Disip4SL30\_2. These stresses are uniformly distributed in all the dissipative windows, indicating a maximum profit of the material. Besides this indicates that the stiffeners do not affect significantly the dissipation.

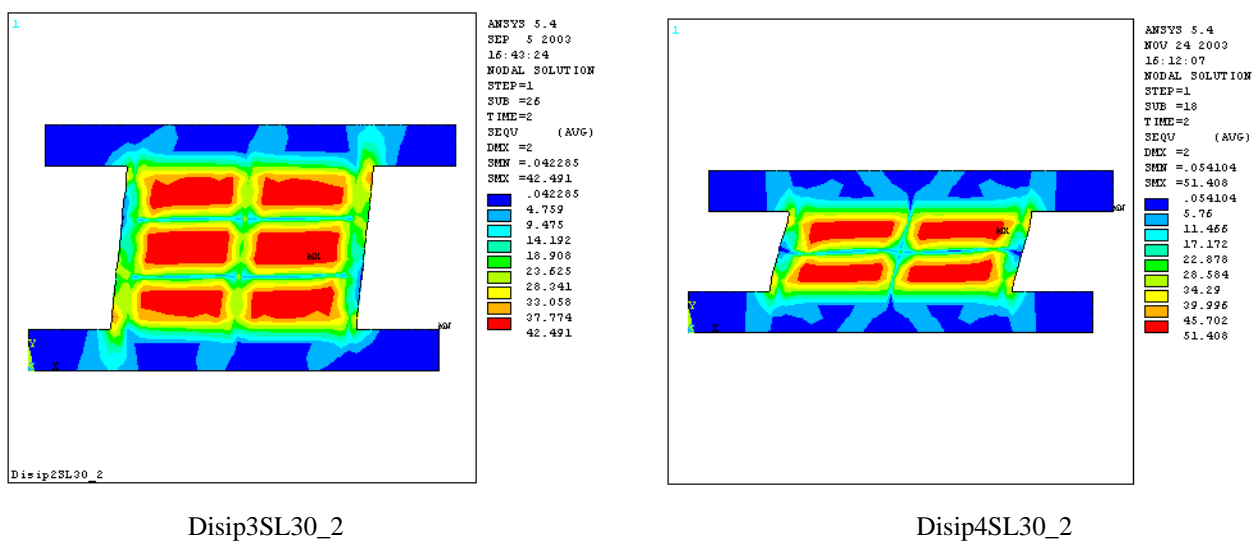
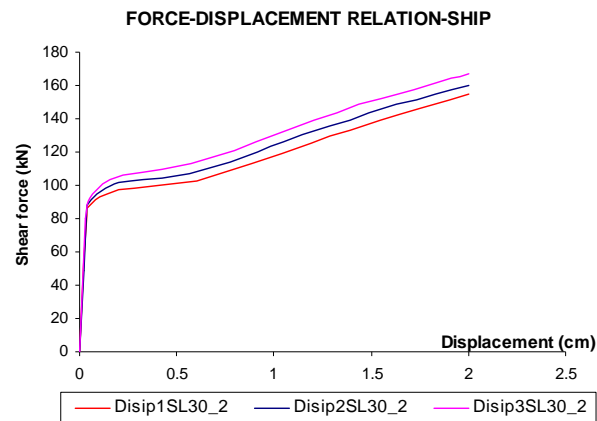


Figure 1. Von Mises stresses for the Disip3SL30\_2 and Disip4SL30\_2 devices.

Figure 2 presents the force–displacement relation-ship for the preliminary 200 mm vertical height proposed devices. The objective is to study the influence of the stiffeners in the yielding strength and post-yielding slope. The increase in stiffeners originates a small increment in the yielding strength, although the post-yielding slope is maintained constant in all the cases. Consequently, the total dissipated energy is increased as the number of stiffeners increases, although the milled area is reduced by them. This result is explained by the stiffness increase. For design purposes, however, all these devices have very similar performances regarding the force–displacement relation-ship.



**Figure 2.** Nonlinear monotonic Force–Displacement relation-ship for the preliminary devices with 200 mm dissipative height.

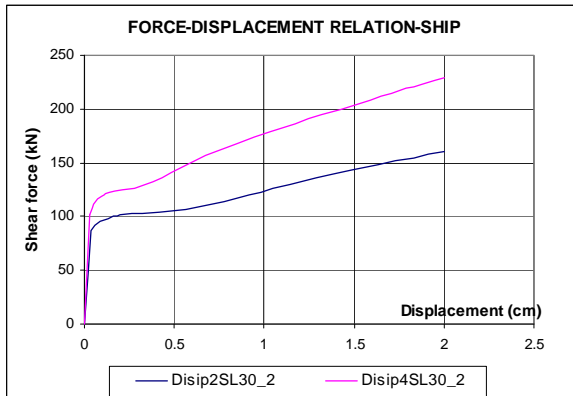
Figure 3(a) presents similar curves but only for the Disip2SL30\_2 (200 mm vertical height) and the Disip4SL30\_2 (110 mm vertical height) preliminary proposed devices. In this case it is notorious the increase in stiffness due to the reduction in vertical dimension. Consequently, the yielding strength is also increased since the yielding displacement is relatively constant among these two preliminary devices. The post-yielding slope is also relatively constant although there is a small increment in stiffness due to the reduction in vertical height. Regarding the dissipated energy it is significantly larger for the stiffer device and this results is explained by demanding a larger deformation capacity in the material.

Figure 3(b) shows the influence of the strain hardening in the monotonic force–displacement relation-ship for device Disip2SL30\_2. The model without hardening shows a small increment in force due to zones that initially do not reach the yielding point. The curve is relatively flat after yielding indicating that the device yields almost completely at the same displacement. This result also indicates that for an imposed 20 mm relative displacement the strains are much larger than the initial yielding one demanding a large deformation capacity.

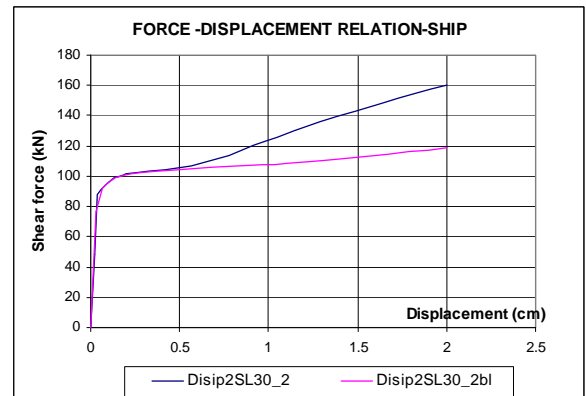
Table 1 summarizes the results from the selection process. Devices Disip1SL30\_2 and Disip2SL30\_2 are disregarded due to web buckling. The dissipators drift during a strong earthquake may be about 10mm, consequently web buckling displacement must be larger than this value. The buckling displacements for these two devices are only 4.98 and 8.95 mm.

Devices Disip3SL30\_2 and Disip4SL30\_2 have initial web buckling displacements of 17.87 and 14.2 mm, respectively. The main advantages of the Disip4SL30\_2 device compared to Disip3SL30\_2 one is its larger stiffness and energy dissipation as well as its smaller milled area. However, these advantages required a larger material ductility. Therefore, the maximum deformation in the device for a 20mm device drift is 0.2902, much larger than the maximum deformation of 0.1515 for the other one. However this material deformation capacity

is available for commercial steel and the maximum 20mm drift considered is double the dissipator working displacement (between 0 to 10mm). Consequently the selected device is the Disip4SL30\_2 called from now on device SL30\_2.



(a)



(b)

**Figure 3.** Monotonic Force–Displacement relation-ship

(a). for devices including one horizontal stiffener but with 110 and 200 mm dissipative height  
(b). for device Disip2SL30\_2 with and without including material hardening.

Table 1. Selection criteria for the dissipators dimensions

SELECTION CRITERION		Disip1SL30_2	Disip2SL30_2	Disip3SL30_2	Disip4SL30_2
1.	Milled area (cm <sup>2</sup> )	500	475	450	250
2.	Number of windows	2	4	6	4
3.	Max. horizontal reactions (kN)	154.54	160.392	167.015	229.296
4.	Max. vertical reactions (kN)	13.064	13.835	14.596	15.152
5.	Maximum strain	0.1437	0.1470	0.1515	0.2902
6.	Maximum shear strain	0.1651	0.1687	0.1749	0.3304
7.	Post-yielding slope	34.986	37.2273	41.3124	64.6584
8.	Initial stiffness (kN/cm)	2,300.35	2,422.05	2,552.15	3,238.60
9.	Dissipated energy (kN.cm)	237	248	260	346
10.	Yielding force (kN)	85.984	87.425	85.853	102.016
11.	Yielding displacement (mm)	0.405	0.40	0.354	0.315
12.	Web buckling displ. (mm)	4.98	8.95	17.87	14.20
13.	Von Mises stresses (kN/cm <sup>2</sup> )	41.342	41.661	42.491	50.069
14.	Max. shear stress (kN/cm <sup>2</sup> )	23.742	24.051	24.530	28.445

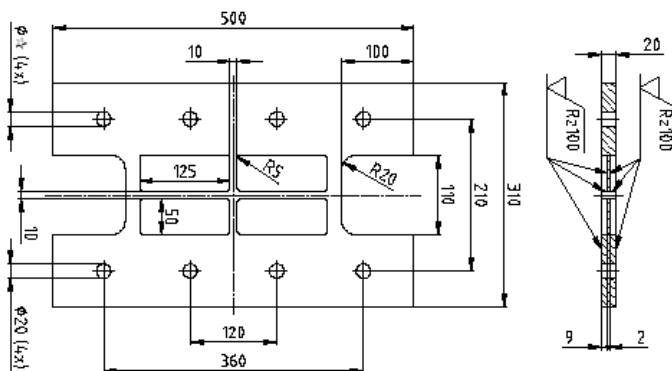


Figure 4. Dimensions for the Disip4SL30\_2 device



Figure 5. Experimental SL30\_2 model tested at ISMES, Italy

#### 4. DESIGN TABLE FOR “SL” DEVICES

As indicated previously the vertical dimension for the proposed SL devices fixes the vertical dimension in 110 mm, including one horizontal stiffener, such as shown in figure 4. These devices are called from this point as SLX\_Y where X denotes the total width and Y denotes the web thickness. The parameter X is varied between 50, up to 500mm and the parameter Y may be 2,3,4 or 5 mm for each given value of X. Consequently there are 32(4x8) different devices under a similar response pattern, providing a large set of nonlinear connections to select from. For example the yielding force among these devices varies from 13.65 kN up to 435.5 kN.

Table 2 presents a summary of the most relevant design parameters for these devices. In order to develop this table a numerical-experimental calibration test was performed at ISMES (Bergamo, Italy) for the device SL30\_2 shown in figure 5. The objective of the test was double fold: (1) calibrate the nonlinear ANSYS model and (2) study the influence of the bolted connection in the hysteretic curves. The experimental tests were cyclic so the monotonic curve shown in figure 6 corresponds to the skeleton of figure 8. Figure 6 shows this numerical-experimental calibration indicating that a good correlation can be obtained using the relatively simple isotropic hardening plasticity model. This is considered an advantage of the device compared to others based on friction or viscous-elastic response that are more difficult to model. For example friction devices are significantly affected by sliding velocity or normal contact pressure. In the other hand viscous devices are affected by temperature. In contrast steel is a material simpler to model and stable under a variety of environmental conditions.

The second experimental objective was more complex since it involved various connection details in order to determine potential fatigue due to continuous loading such as wind. The bolts were all 20 mm diameter but their prestressing force or the dimensions of the holes were varied from 21, 22 and 24 mm. Cycling tests were performed to obtain hysteretic curves and fatigue ones.

Figures 7 and 8 shows the hysteretic curves for the connection with the smallest tolerance, i.e. 21mm holes. The figure 7 includes the slippage in the connection while the curve in 8 do not include any slippage (This indicates that the first curve is obtained using displacement transducers above the holes and the second curve within the holes and consequently do not including the slipping of the bolts). The experimental yielding force was about 150 kN and the yielding displacement about 0.5-1 mm. The total cumulative dissipated energy before any degrading of the devices was 77.528 kN.mm and 53.851 kN.mm for the first and second curves, respectively. For the second case the total dissipated energy after degradation of the device, i.e. including the flexure mode, was 97.210 kN.mm. This indicates that a significant additional energy may be attained by the flexural mode as well as by the slipping of the connection. However, slippage is not considered a good response characteristic since it is difficult to predict. Consequently the tolerance is reduced as much as possible just for installing the devices.

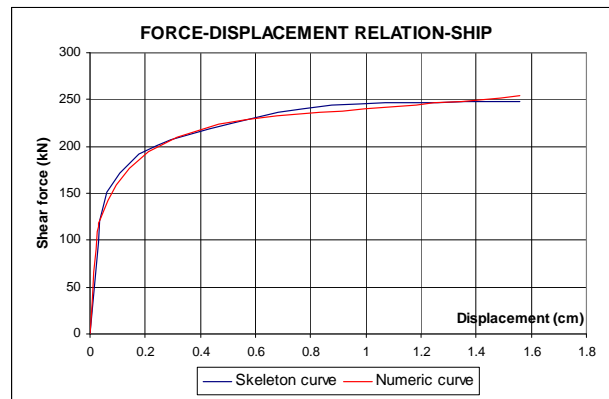


Figure 6. Experimental and numerical monotonic Force-Displacement relation-ship for device SL30\_2

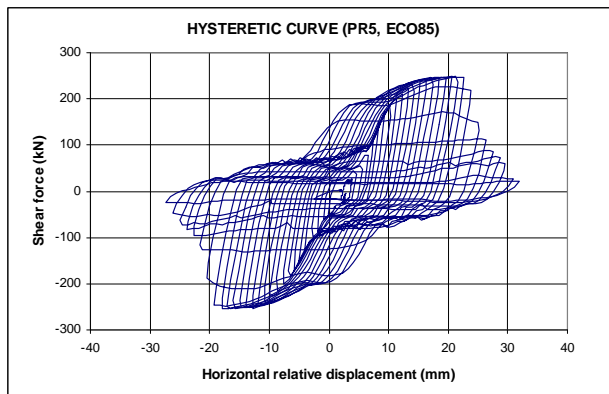


Figure 7. Hysteretic curve for device SL30\_2 including slippage of the bolts

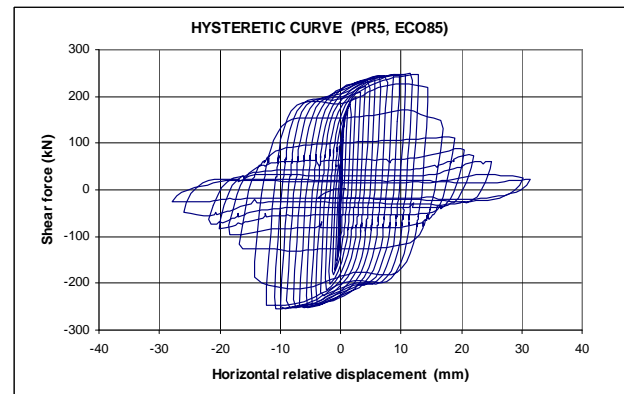


Figure 8. Hysteretic curve for device SL30\_2 without slippage of the bolts

Regarding fatigue due to repetitive loading such as wind, it was observed but after a large number of cycles even for a large imposed displacement. This was a quite surprising result since initially it was estimated that a small number of cycles in  $\pm 10$ mm range should cause fatigue. Experimentally it was observed that even with this large drift the number of cycles was more than one hundred. This result is explained by the slippage of the bolted connections that reduced the plastic strain in the devices significantly, particularly after the initial cycles. The experimental failure mode was fatigue of the bolted vertical connections that attached the devices to the testing machine. Due to experimental set up restrains these bolts were welded to a horizontal plate filling the 21 mm holes. This weld failed after a large number of cycles most probably by the continuous impact caused by the slippage of the bolts in the holes. Taking into account that the drift due to wind loads will be much smaller than 10 mm it can be concluded from the tests that fatigue is not a concern in these devices, at least, providing a minimum 1mm hole tolerance. The devices are usually installed after completing the construction of the structure, so they do not carry any significant vertical load. Consequently due to building deformations tolerance is always necessary for installing the devices.

Table 2. The most relevant design parameters for the devices

Device	e	K <sub>1</sub> (KN/cm)	K <sub>2</sub> (KN/cm)	d <sub>y</sub> (mm)	f <sub>y</sub> (kN)	D <sub>y</sub> (mm)	F <sub>y</sub> (kN)	F <sub>max</sub> (kN)	D <sub>a</sub> (mm)	E <sub>d</sub> (KN.cm)
SL5_2	2	546,1	14,4	0,250	13,65	0,463	25,27	47,32	39,93	54
SL5_3	3	663,5	13,4	0,321	21,30	0,549	36,40	56,59	89,87	69
SL5_4	4	763,8	11,8	0,357	27,27	0,628	47,96	65,26	159,83	84
SL5_5	5	834,3	8,8	0,357	29,78	0,716	59,76	72,93	249,81	97
SL10_2	2	1 273,8	22,1	0,250	31,85	0,437	55,68	89,56	29,81	109
SL10_3	3	1 644,4	21,6	0,277	45,55	0,491	80,67	113,62	67,10	146
SL10_4	4	1 979,1	20,1	0,304	60,16	0,540	106,86	136,91	119,35	182
SL10_5	5	2 216,7	17,4	0,331	73,26	0,600	133,00	159,27	186,45	216
SL15_2	2	2 285,9	22,4	0,250	57,15	0,567	129,60	163,04	20,29	216
SL15_3	3	2 929,6	23,3	0,268	78,51	0,565	165,55	200,32	45,66	271
SL15_4	4	3 493,5	22,9	0,286	99,91	0,573	200,20	236,30	81,18	325
SL15_5	5	3 856,1	22,3	0,321	123,78	0,618	238,33	271,48	126,85	377
SL20_2	2	2 971,2	24,1	0,250	74,28	0,536	159,18	195,36	15,96	262
SL20_3	3	3 980,0	24,9	0,268	106,66	0,527	209,68	247,72	35,92	339
SL20_4	4	4 719,3	25,8	0,286	134,97	0,553	261,00	298,88	63,85	414
SL20_5	5	5 262,7	24,0	0,321	168,93	0,596	313,46	349,12	99,77	489
SL25_2	2	3 660,6	24,3	0,250	91,51	0,514	188,18	224,74	14,44	305
SL25_3	3	4 859,0	25,2	0,268	130,22	0,524	254,52	292,09	32,50	404
SL25_4	4	5 921,3	24,7	0,286	169,35	0,544	321,82	358,05	57,79	501
SL25_5	5	6 613,5	24,5	0,321	212,29	0,588	389,20	423,17	90,30	597
SL30_2	2	4 353,6	24,5	0,250	108,84	0,497	216,56	253,78	13,75	348
SL30_3	3	5 791,0	25,5	0,268	155,20	0,513	297,22	336,02	30,93	468
SL30_4	4	7 129,9	25,4	0,286	203,91	0,531	378,46	416,81	54,99	587
SL30_5	5	7 981,8	25,2	0,321	256,21	0,575	459,17	496,73	85,92	704
SL40_2	2	5 820,4	30,9	0,250	145,51	0,490	285,12	331,02	14,02	455
SL40_3	3	7 778,5	32,0	0,268	208,46	0,507	394,44	442,74	31,55	619
SL40_4	4	9 621,2	33,1	0,286	275,17	0,523	503,33	553,98	66,90	781
SL40_5	5	10 777,4	31,8	0,321	345,95	0,570	614,29	662,15	104,53	941
SL50_2	2	7 223,6	32,9	0,250	180,59	0,473	342,00	391,08	13,40	542
SL50_3	3	9 703,1	35,9	0,268	260,04	0,495	480,00	533,58	30,16	749
SL50_4	4	12 109,3	32,7	0,286	346,33	0,514	622,22	671,76	53,62	954
SL50_5	5	13 566,7	31,0	0,321	435,49	0,563	764,00	810,65	83,79	1160

K<sub>1</sub>, Initial stiffness  
K<sub>2</sub>, Post-yielding stiffness  
d<sub>y</sub>, Initial yielding displacement  
f<sub>y</sub>, Initial yielding force  
D<sub>y</sub>, Yield displacement

F<sub>y</sub>, Yield force  
F<sub>max</sub>, 1.559 cm displacement force to  
D<sub>a</sub>, Web buckling displacement  
e, Milled area thickness  
E<sub>d</sub>, Dissipated energy

## 5. CONCLUSIONS

In this study the device proposed has an excellent capacity of energy dissipation that basically is carried out through inelastic strain of the web and it is characterized for uniform stress distribution in the dissipative area, which is similar to the distribution of shear stresses in the web of a wide-flange section.

The device works in a double mode. Initially the energy is mainly dissipated in the web by uniform shear stresses in a shear mode. After the web degrades the stiffeners continue dissipating energy in a flexural mode, leading to a robust system that continues dissipating energy even after the web degradation.

The calibration of the force-displacement relationship of the numeric model with respect to the backbone of the experimental model showed a good correlation using a relatively simple isotropic hardening plasticity model. This is an advantage of the device compared to other devices based on friction or viscous-elastic response that are more difficult to model. All the devices yielded at very low displacements on the order of 0.25 - 0.35 mm while the yielding forces varied between 13.65 and 435.5 kN with associated dissipated energy between 54 and 1160 kN.cm respectively.

This device can be used for seismic protection of existing buildings or for providing ductility to new buildings.

Using the design chart presented in this paper, it is relatively simple to analyze buildings equipped with this type of hysteretic connections, under seismic excitations.

## 6. REFERENCES

- Bozzo, L.M., Cahís, X. y Torres, L.I. (1998). A shear type energy dissipator for the protection of masonry infill walls. *Proceedings of the Sixth U.S. National Conference on Earthquake Engineering*: Seattle, Washington.
- Bozzo, L. and Barbat A. (1999), Diseño sismorresistente de edificios. Técnicas convencionales y avanzadas, Editorial Reverte, Barcelona.
- Cahís X, Torres L.I, Bozzo L. (2000). An innovative elasto-plastic energy dissipator for the structural and non-structural building protection. *12<sup>th</sup> World Conference on Earthquake Engineering*: Auckland, New Zealand.
- Hurtado S. F. (2006). Propuesta de disipador genérico "SL" para edificios y su diseño sismorresistente. Tesis Doctoral, Barcelona.
- Kasai, K. and Popov, E.P. (1986). Cyclic web buckling control for shear link beams. *Journal of Structural Engineering*, ASCE: **110(3)**, 505-523.
- Rai, D.C. and Wallace, B.J.(1998). Aluminium Shear-links for enhance seismic resistance. *Earthquake Engineering and Structural Dynamics*: **27**,315-342.
- Roeder, C.W., and Popov, E.P. (1977). Inelastic behavior of eccentric braced steel frames under cyclic loadings. *EERC Report no. 77-18, Earthquake Engineering Research Center, University of California, Berkeley.*